Double parametric resonance for matter-wave solitons in a time-modulated trap

Bakhtiyor Baizakov,[1] Giovanni Filatrella,[2] Boris Malomed,[3] and Mario Salerno[1]
[1]*Dipartimento di Fisica "E. R. Caianiello" and Istituto Nazionale di Fisica della Materia (INFM), Università di Salerno, I-84081 Baronissi (SA), Italy*
[2]*INFM, Laboratorio Regionale di Salerno and Dipartimento di Scienze Biologiche ed Ambientali, Università del Sannio, via Port'Arsa 11, 82100 Benevento, Italy*
[3]*Department of Interdisciplinary Studies, Faculty of Engineering, Tel Aviv University, Tel Aviv 69978, Israel*
(Received 17 June 2004; published 23 March 2005)

We analyze the motion of solitons in a self-attractive Bose-Einstein condensate, loaded into a quasi-one-dimensional parabolic potential trap, which is subjected to time-periodic modulation with an amplitude ε and frequency Ω. First, we apply the variational approximation, which gives rise to decoupled equations of motion for the center-of-mass coordinate of the soliton, $\xi(t)$, and its width $a(t)$. The equation for $\xi(t)$ is the ordinary Mathieu equation (ME) (it is an exact equation that does not depend on the adopted ansatz), the equation for $a(t)$ being a nonlinear generalization of the ME. Both equations give rise to the same map of instability zones in the (ε,Ω) plane, generated by the parametric resonances (PRs), if the instability is defined as the onset of growth of the amplitude of the parametrically driven oscillations. In this sense, the double PR is predicted. Direct simulations of the underlying Gross-Pitaevskii equation give rise to a qualitatively similar but quantitatively different stability map for oscillations of the soliton's width $a(t)$. In the direct simulations, we identify the soliton dynamics as unstable if the instability (again, realized as indefinite growth of the amplitude of oscillations) can be detected during a time comparable with, or smaller than, the lifetime of the condensate (therefore accessible to experimental detection). Two-soliton configurations are also investigated. It is concluded that multiple collisions between solitons are elastic, and they do not affect the instability borders.

DOI: 10.1103/PhysRevE.71.036619 PACS number(s): 05.45.Yv, 03.75.Kk, 03.75.Lm

I. INTRODUCTION

The experimental observations of solitons in effectively one-dimensional (1D) Bose-Einstein condensates (BECs) with attractive interactions between atoms [1,2] make the study of soliton dynamics in this medium a highly relevant subject. In a permanent form, solitons can be created in a "cigar-shaped" condensate, subjected to tight transverse and loose longitudinal trapping; see, e.g., a relevant discussion in Ref. [3] and references therein. The soliton may perform harmonic oscillations, as a quasiparticle, in a trap with a longitudinal parabolic potential profile (in more sophisticated settings, including an additional optical lattice periodic potential, and also the possibility of repulsive interactions between atoms in the condensate, the oscillatory motion of one- and two-dimensional BEC solitons was studied in detail in the recent works [4,5], respectively). Thus a natural way to test various dynamical properties of the system (in particular, manifestations of possible resonances) is to use a magnetic trap whose strength is periodically modulated in time [6,7]. This can be readily implemented by applying a mixture of dc and ac magnetic fields to the condensate. Another possibility would be the periodic modulation of the nonlinear coefficient through the atomic *s*-wave scattering length. Resonances in spherically symmetric trapped Bose-Einstein condensates under a periodically varying atomic scattering length were considered in a recent paper [8].

The motion of a soliton in a 1D trap with time-modulated strength is an issue of straightforward interest for realization in experiments. Recently, this problem was considered in Ref. [9] for the case of rapid modulation with a large frequency Ω. For this case, an effective equation of motion was derived by means of an averaging procedure, which, in particular, predicts the possibility of a stable equilibrium in an inverted trap, corresponding to a negative sign in front of the potential term in the Gross-Pitaevskii equation (GPE) (4) (see below). The existence of such a state was corroborated by direct simulations of the full equation. However, parametric resonances (PRs), which are the subject of the present work, were not dealt with in Ref. [9], as the resonance cannot take place in the large-Ω limit. Resonances in collective oscillations of a 1D *repulsive* BEC due to periodic modulation of the nonlinear coefficient and trap frequency were investigated in [10], in both the high density limit described by the mean-field GPE, and the low density Tonks-Girardeau regime described by the nonlinear Schrödinger equation with quintic nonlinearity.

In this work, we aim to study PRs in the motion of solitons in a 1D condensate with *attractive* nonlinearity. Obviously, the most interesting situation is that when mean-field effects, accounted for by the GPE in its capacity of a partial differential equation (PDE), can alter the resonances, if compared to the relatively simple approximation which amounts to an ordinary differential equation (ODE) [in particular, the Mathieu equation (ME)]. In this sense, the PR in the motion of the soliton's center of mass is of lesser interest, as the corresponding ODE is an exact equation, decoupled from PDE effects [6] (the Ehrenfest theorem). A more promising direction is to study resonant effects in internal vibrations of the soliton, as in this case the corresponding ODE is only an approximation. Besides that, in the latter case the PRs will be resonances in a truly nonlinear system, as the corresponding ODE is a nonlinear one. This, in effect, implies the consideration of a double parametric resonance: it will be demonstrated below that PR-induced instabilities set in simultaneously in the ODEs describing the evolution of the soliton's width and center-of-mass position.

Actually, the onset of the instability, in the form of permanent growth of the amplitude of parametrically driven oscillations, is the most important manifestation of the PR. Accordingly, in the case of the ME, if it is cast in the from of Eq. (13) (see below), the PRs of different orders $n=1,2,\ldots$ generate well-known instability zones in the plane of (Ω,ε), at values close to $\Omega_{\mathrm{PR}}^{(n)}=2\sqrt{2}/n$ [11]. The main result of the present work will be summarized in the form of a similar but quantitatively different map of instability zones for intrinsic vibrations of the soliton and oscillations of its center of mass, found from direct simulations of the GPE (4). The double PR takes place in the overlapping regions of the two zones.

The analysis developed in this work has common features with the study of intrinsic oscillations in the three-dimensional (3D) BEC with *repulsive* nonlinearity, trapped in a parabolic potential with time-modulated strength. This problem was considered in Refs. [6] and [8], which also employed the variational approximation (VA) to predict the evolution of the condensate's size. The corresponding equation derived in Ref. [6] for the radial size $a(t)$ of the condensate differs from our Eq. (10), derived below for the soliton's size, by an opposite sign in front of the term proportional to N, and by its power (it was $\sim a^{-4}$, due to the 3D character of the problem considered in [6]). In that work, an instability map was drawn only on the basis of the ODE results. Here we present the PDE-based map (and the model is different, due to the different dimension and the attractive sign of the nonlinearity).

The rest of the paper is organized as follows. In Sec. II we describe the model and derive the variational equations. Section III presents basic results for the PR in the dynamics of a soliton trapped in a time-modulated parabolic potential. In Sec. IV, we consider a configuration with two identical solitons created in the trap, concluding that multiple collisions between the solitons do not inflict any damage on them. The paper is concluded by Sec. V.

II. THE MODEL AND VARIATIONAL APPROXIMATION

The dynamics of a BEC in the mean-field approximation at zero temperature is governed by the 3D GPE

$$i\hbar\frac{\partial\Psi}{\partial t}=\left[-\frac{\hbar^2}{2m}\nabla^2+V(x,y,z)+\frac{4\pi\hbar^2a_sN}{m}|\Psi|^2\right]\Psi, \quad (1)$$

where $\Psi(\mathbf{r},\mathbf{t})$ is the macroscopic wave function of the condensate normalized so that $\int|\Psi(\mathbf{r})|^2d\mathbf{r}=1$, N is the total number of atoms, m is the atomic mass, a_s is the s-wave scattering length (below we shall be concerned with an attractive BEC for which $a_s<0$), and

$$V(x,y,z)=\frac{m}{2}[\omega_x^2x^2+\omega_\perp^2(y^2+z^2)] \quad (2)$$

is the axially symmetric trapping potential which provides for tight confinement in the transverse plane (y,z), as compared to loose axial trapping, assuming $\omega_x^2/\omega_\perp^2\ll 1$. The condensate trapped in such a potential acquires a highly elongated form (cigar shape).

When the transverse confinement is strong enough, so that the transverse oscillation quantum $\hbar\omega_\perp$ is much greater than the characteristic mean-field interaction energy per particle $N|a_s||\Psi|^2$, the dynamics is effectively one dimensional. In this case, the wave function may be effectively factorized as $\Psi(x,y,z,t)=\psi(x,t)\phi(y,z)$, where $\phi(y,z)=\exp[-(y^2+z^2)/2a_\perp^2]/\sqrt{\pi}a_\perp$ is the normalized ground state of the 2D harmonic oscillator in the transverse direction, with $a_\perp=\sqrt{\hbar/m\omega_\perp}$ being the corresponding transverse harmonic-oscillator length. Inserting the factorized expression into the 3D GPE (1), and integrating it over the transverse plane (y,z), one derives the effective 1D GPE [12]

$$i\hbar\frac{\partial\psi}{\partial t}=\left[-\frac{\hbar^2}{2m}\frac{\partial^2}{\partial x^2}+\frac{m}{2}\omega_x^2x^2+g_{1\mathrm{D}}N|\psi|^2\right]\psi, \quad (3)$$

where we have neglected the zero-point energy of the transverse motion $\hbar\omega_\perp$, and defined the coefficient of the 1D nonlinearity, $g_{1\mathrm{D}}=4\pi\hbar^2a_sm^{-1}\int|\phi(y,z)|^4dy\,dz=2a_s\hbar\omega_\perp$. Essentially the same 1D equation can be derived in another situation, when the nonlinearity is much larger than the transverse kinetic energy [13].

We now assume the axial parabolic trap to be time dependent $\sim f(t)x^2$, and rewrite Eq. (3) using the dimensionless variables $t\to\omega_xt$, $x\to x/a_x$, $a_x=\sqrt{\hbar/m\omega_x}$, and the rescaled wave function $\psi\to\sqrt{2N|a_s|\omega_\perp/a_x\omega_x}\psi$,

$$i\frac{\partial\psi}{\partial t}+\frac{1}{2}\frac{\partial^2\psi}{\partial x^2}-f(t)x^2\psi+|\psi|^2\psi=0, \quad (4)$$

$$f(t)\equiv 1+\varepsilon\cos(\Omega t), \quad (5)$$

where the strength of the constant ("dc") parabolic trap is scaled to be 1, ε and Ω being the amplitude and frequency of the time-dependent ("ac") part of the trap's strength. The amplitude, which is defined to be positive, obeys the obvious restriction $\varepsilon\leqslant 1$, as we do not consider the case of an expulsive potential.

To estimate actual values of the time and space units, we take the experimental parameters from Ref. [2]. In this experiment, a single soliton in a ^{7}Li condensate of $N=4\times10^3$ atoms was created in an axially symmetric parabolic trap with $\omega_\perp=2\pi\times710$ Hz and $\omega_x=2\pi\times50$ Hz (subsequently, the axial potential was made expulsive, which formally corresponds to an imaginary confining frequency $\omega_x=2\pi i\times78$ Hz). The s-wave scattering length, at the value of the magnetic field $B=420$ G (which was used to make the atomic interaction attractive, via the Feshbach resonance), was $a_s=-0.21$ nm. With the mass of a ^{7}Li atom, $m=11.65\times10^{-27}$ kg, we have the following time and space units: $\omega_x^{-1}\simeq3\times10^{-3}$ s, $a_x=\sqrt{\hbar/m\omega_x}\simeq12$ μm, the trap's aspect ratio being $\omega_x/\omega_\perp\simeq7\times10^{-2}$.

As is well known, there is a drastic difference in the stability between the 3D and 1D attractive condensates, as collapse occurs in the 3D case at a critical value of the parameter $k=N|a_s|/a_{\mathrm{HO}}$ (a_{HO} is the harmonic-oscillator length characterizing the strength of the magnetic trap), corresponding to a situation when the attractive forces overwhelm the kinetic energy, and the condensate rapidly shrinks. For instance, in isotropic 3D traps ($\omega_x=\omega_\perp=\omega_0$, $a_{\mathrm{HO}}=\sqrt{\hbar/m\omega_0}$), the Gaussian ansatz for the wave function predicts collapse at $k_{\mathrm{cr}}=N|a_s|/a_{\mathrm{HO}}=0.671$ [14], while direct numerical solution of the GPE (1) yields $k_{\mathrm{cr}}\simeq 0.575$ [15]. In a waveguide trap without longitudinal confinement ($\omega_x=0$), the collapse occurs at a slightly different value $k_{\mathrm{cr}}=N|a_s|/a_\perp=0.627$, which was found by applying the imaginary-time relaxation method to the GPE (1) [16]. Unlike *strong* 3D collapse, *weak* collapse in the 2D GPE occurs if the peak density exceeds a critical value $(|\psi|^2)_{\mathrm{cr}}=11.7/(8\pi N|a_s|/a_\perp)$ [3]. In the present work, simulations of the 1D equation (4) were run for values of the parameters that ensure the absence of transverse (2D) or 3D collapse in the full underlying 3D system.

Numerical simulations of Eq. (4) were performed by means of two versions of the operator-splitting technique: (i) using fast Fourier transform [17] and (ii) with the Crank-Nicholson scheme [18]. These two numerical methods produced practically identical results. We employed a finite domain $-L\leqslant x\leqslant L$, with absorbers installed near the edges to prevent reentering of a small amount of linear waves emitted by the perturbed soliton. The domain length $2L$ was sufficient to detect indefinite growth (at least by a factor of ten) of amplitudes of oscillations of the soliton's center-of-mass coordinate and width due to the parametric resonances.

In the absence of the potential term $f(t)=0$, Eq. (4) gives rise to a commonly known family of soliton solutions,

$$\psi_{\mathrm{sol}}(x,t) = \eta\,\mathrm{sech}[\eta(x-\xi)]\exp\left\{\frac{i}{2}[(\eta^2-\dot{\xi}^2)t+\dot{\xi}x]\right\}, \quad (6)$$

where ξ and $\dot{\xi}$ are, respectively, the instantaneous coordinate and velocity of the soliton's center, while the amplitude η determines the number of atoms (norm) of the condensate,

$$N_s \equiv \int_{-\infty}^{+\infty}|\psi(x)|^2dx = 2\eta, \quad (7)$$

which is the single dynamical invariant of Eq. (4) with the time-dependent coefficient $f(t)$. The norm N_s is connected to the "real" number of atoms N in the original 3D GPE (1) as

$$N_s = 2N\frac{|a_s|\omega_\perp}{a_x\omega_x}. \quad (8)$$

For the above mentioned experimental settings of [2] the relation is $N_s\simeq 1.115\times 10^{-3}N$, so that approximately $N=900$ atoms needed to have the norm of the soliton $N_s=1$ used in our numerical simulations.

The soliton's dynamics in the trapping potential can also be described by means of the variational approximation, which is a well-known tool for the consideration of solitons in nonintegrable models [19]. In particular, the VA for the three-dimensional GPE with repulsive nonlinearity and time-modulated strength of the trap was elaborated in Ref. [6]. In this work, we adopt the following ansatz for a perturbed 1D soliton:

$$\psi(x,t) = \eta\,\mathrm{sech}\left(\frac{x-\xi}{a}\right)\exp\{i[\phi+w(x-\xi)+b(x-\xi)^2]\}, \quad (9)$$

where η, a, ξ, ϕ, w, and b are time-dependent real variational parameters. The norm (7) corresponding to the ansatz (9) is $N_s=2\eta^2a$. The subsequent derivation is straightforward, ending up with a system of dynamical equations for the soliton's width and coordinate:

$$\ddot{a} = \frac{4}{\pi^2a^3} - \frac{2N_s}{\pi^2a^2} - 2f(t)a, \quad (10)$$

$$\ddot{\xi} = -2f(t)\xi, \quad (11)$$

where the overdot stands for d/dt. The other dynamical variables are related to these by $w=\dot{\xi}$ and $b=\dot{a}/(2a)$.

Equation (10) was previously considered in the context of disintegration of optical solitons in fibers with randomly varying parameters [20], and recently with regard to collective oscillations of a 1D repulsive BEC under time-varying trap potential and nonlinearity [10]. Equations similar to (10) and (11) can also be obtained by means of the moment method for the evolution of an optical beam in a system of nonlinear graded-index fibers [21]. In that work, strong resonances in the beamwidth oscillations were found, when the fiber's graded index is a piecewise-constant periodic function of the propagation coordinate.

The fact that Eq. (11) for ξ is decoupled from the other one is a general result, which is valid irrespective of the applicability of the VA. Indeed, Eq. (11) for the soliton's center-of-mass coordinate, which is defined as

$$\xi(t) \equiv N_s^{-1}\int_{-\infty}^{+\infty}x|\psi(x,t)|^2dx, \quad (12)$$

where N_s is the conserved norm (7), can be derived as an *exact* corollary of the GPE with a (time-dependent) parabolic potential [6]. In fact, this is the Ehrenfest theorem in the present context (its validity for the nonlinear Schrödinger equation with a parabolic potential was proved in Ref. [22]).

In the case of a harmonic time modulation of the trap's strength as per Eq. (5), the equation of motion (11) for the soliton's center is the Mathieu equation [11],

$$\ddot{\xi} + 2[1+\varepsilon\cos(\Omega t)]\xi = 0. \quad (13)$$

As is commonly known, the ME gives rise to parametric resonances when Ω is close to the values

$$\Omega_{\mathrm{PR}}^{(n)} = 2\sqrt{2}/n, \quad (14)$$

$n=1$ and $n>1$ (n is integer) corresponding to the fundamental and higher-order resonances, respectively. In fact, Eq. (10) with the function $f(t)$ taken from Eq. (5) may be regarded as a nonlinear generalization of the ME, which also gives rise to PRs.

It is relevant to mention that, in the low-density limit ($N_s\ll\pi^2a^2/2$), the second term on the right-hand side of Eq. (10) can be dropped. Such a simplified equation is equivalent to an *exact* equation for the width, which was derived in Ref.

[7] (without the use of the VA or other approximation) from the two-dimensional GPE with repulsive nonlinearity and parabolic trapping potential. It is known that solutions of the latter equation can be expressed, also in an exact form, in terms of solutions of the linear ME. Therefore, in the limit when the underlying GPE (4) goes over into the linear Schrödinger equation, which corresponds to $a_s=0$, the PRs in Eq. (10) are exactly the same as in Eq. (11). However, Eq. (10) cannot be reduced to the linear ME in the general case ($a_s \neq 0$).

III. INSTABILITY ZONES FOR THE TRAPPED SOLITON

A. The soliton in the time-independent trap and nonresonant motion in the time-modulated one

First, we test the accuracy of the VA, which was briefly described above, in the dc case, i.e., with $\varepsilon=0$ in Eq. (4). As mentioned above, the equation for $\xi(t)$ is independent of the adopted ansatz, in compliance with the Ehrenfest theorem. By contrast, Eq. (10) for the width of a soliton $a(t)$ stems from the VA with the ansatz (9). The latter equation coincides with one for a unit-mass particle in the potential

$$U(a) = \frac{2}{\pi^2 a^2} - \frac{2N_s}{\pi^2 a} + f(t)a^2.$$

In the dc case, $f(t)\equiv 1$, the value of the width a of a stationary soliton corresponds to the minimum of this potential, which is determined by the real positive root of the equation

$$a^4 + \frac{N_s}{\pi^2}a - \frac{2}{\pi^2} = 0. \tag{15}$$

Obviously, when the first term in this equation may be neglected, we have a prediction for the width of a soliton coinciding with that in Eqs. (6) and (7), $a=1/\eta=2/N_s$. Therefore, the VA is more accurate for a soliton whose width is narrow in comparison with the harmonic-oscillator length of the parabolic trap. For instance, at $N_s=5$ we have $a=0.37$ from Eq. (15), which is close to $a=0.4$ following from the full equation (7).

In direct simulations of the GPE (4), the initial condition was taken as the soliton (6) with some off-center displacement ξ_0 and zero velocity: $\psi_0(x)=\eta\,\mathrm{sech}[\eta(x-\xi_0)]$. Then, the soliton's coordinate, as a function of time, was extracted from a numerical solution of Eq. (4) as per the definition (12), and the width $a(t)$ was identified as follows:

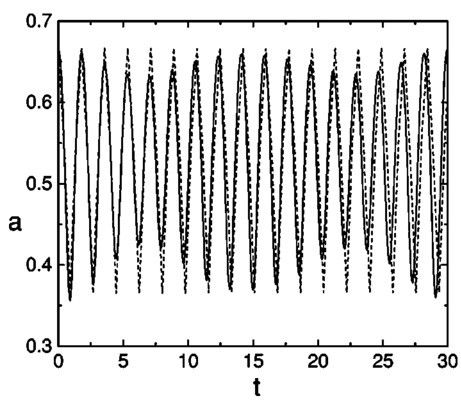

FIG. 1. Evolution of the width $a(t)$ of the relatively broad soliton (6), with the initial amplitude $\eta_0=1.5$, off-center shift $\xi_0=0.3$, and zero initial velocity, in the model with a dc parabolic trap ($\varepsilon=0$). In this figure and below, the solid and dashed lines show, respectively, the results obtained from direct simulations of the GPE (4), and from numerical solutions of Eqs. (10) and (11).

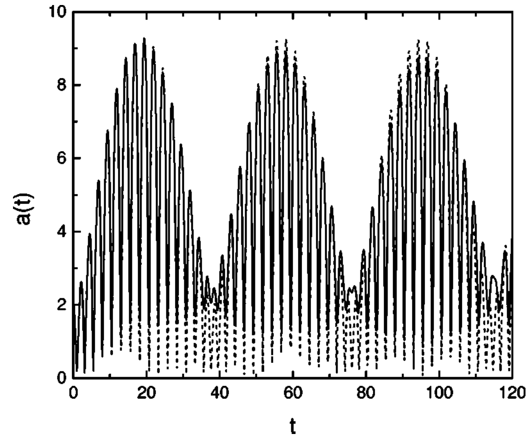

FIG. 2. Nonlinear oscillations of the soliton's width, in the case of temporal modulation of the parabolic trap's strength moderately close to the parametric resonance, with $f(t)=1+\varepsilon\cos(\Omega t)$, $\varepsilon=0.5$, and $\Omega=2.43$. The initial condition is $\psi_0(x)=\eta_0\,\mathrm{sech}[\eta_0(x-\xi_0)]$ with $\eta_0=0.5$ and $\xi_0=1.0$. The solid and dashed lines correspond, respectively, to the simulations of the PDE (4) and ODE (10).

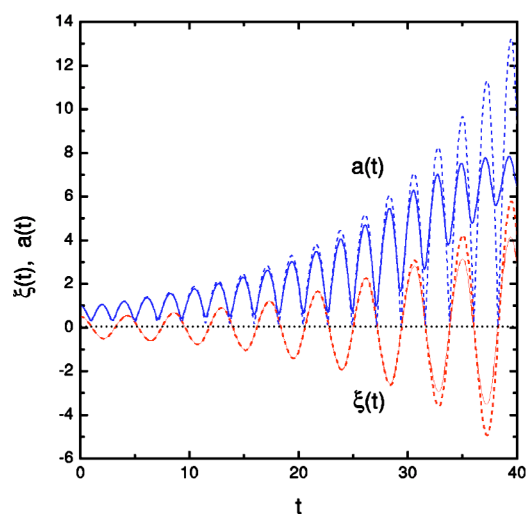

FIG. 3. A double parametric resonance shows up as simultaneous permanent growth of the amplitudes of oscillations of $\xi(t)$ and $a(t)$. Numerical simulations of the GPE (4) with the initial condition $\psi_0(x)=\eta_0\,\mathrm{sech}[\eta_0(x-\xi_0)]$, where $\eta_0=1.0$ and $\xi_0=0.5$, are compared to numerical solutions of ODEs (10) and (11). The harmonic trap is periodically modulated at the fundamental-resonance frequency $\Omega=2\sqrt{2}$, with the amplitude $\varepsilon=0.2$. The thick and thin continuous lines refer to PDE simulations, while corresponding dashed lines refer to ODE simulations.

$$a^2(t) \equiv N_s^{-1}\int_{-\infty}^{+\infty}[x-\xi(t)]^2|\psi(x,t)|^2dx \qquad (16)$$

[recall that N_s is the conserved norm of the solution defined in Eq. (7)].

If the initial soliton is narrow [$a(0) \ll 1$, $\dot{a}(0)=0$], integration of Eq. (10) yields $a(t)$ which is virtually identical to that following from the solution of Eq. (4), with regard to the definition (16). However, for $a(0)\sim 1$, i.e., for a broader soliton, the discrepancy between the ODE and PDE results is notable, as is illustrated by Fig. 1.

Next, we compare the evolution of the soliton's width $a(t)$ in a trap including an ac part ($\varepsilon \neq 0$), but still not very close to the PR, as found from the solution of the variational Eq. (10), and from the full PDE simulations as per Eq. (16). A typical example of the comparison is displayed in Fig. 2.

As may be expected in a nonlinear system, periodic forcing with a frequency close to the resonance results in complex dynamics. The frequency of the oscillations depends on the amplitude, which leads to detuning the system from the resonance as the amplitude grows. The periodic slow dynamics of the amplitude in Fig. 2 is a manifestation of this phenomenon (which is usually called a nonlinear resonance [23]). This general character of the evolution is qualitatively similar in the ODE and PDE results; some discrepancy between them is explained by a deformation of the soliton performing the oscillations with a large amplitude in the parabolic trap [in the case shown in Fig. 2, the maximum amplitude of the oscillations of $\xi(t)$ is ≈ 4.5]. The deformation breaks the symmetry of the soliton's shape, which was assumed in the ansatz (9); hence Eq. (10), which was derived from the symmetric ansatz, may become inaccurate. Despite the intrinsic vibrations, the soliton oscillating in the parabolic trap, whose strength is periodically modulated in time, remains completely stable in this regime.

B. The double parametric resonance

As was mentioned above, the trivial solution $\xi \equiv 0$ of the ME loses its stability in certain zones in the parameter plane (Ω, ε) close to the PR points (14) [11]. In that case, $\xi(t)$ features oscillations with a permanently growing amplitude. The solution of Eq. (10), which is a nonlinear generalization of the ME, is always an oscillatory one, and it may be expected that, also close to the points (14), a periodic solution will develop an instability that will also manifest itself in the unlimited growth of the amplitude of the oscillations. This expectation is corroborated by simulations of Eq. (10). As was explained in the Introduction, we always identify the PR-induced instability as a permanent growth of the amplitude of oscillations in simulations of the corresponding equation, and this definition makes the onset of the instability in Eqs. (11) and (10) identical. Thus, a *double parametric resonance* takes place in the system.

In direct simulations of the full GPE (4), double PR is observed indeed, in the form of growth of the amplitude of

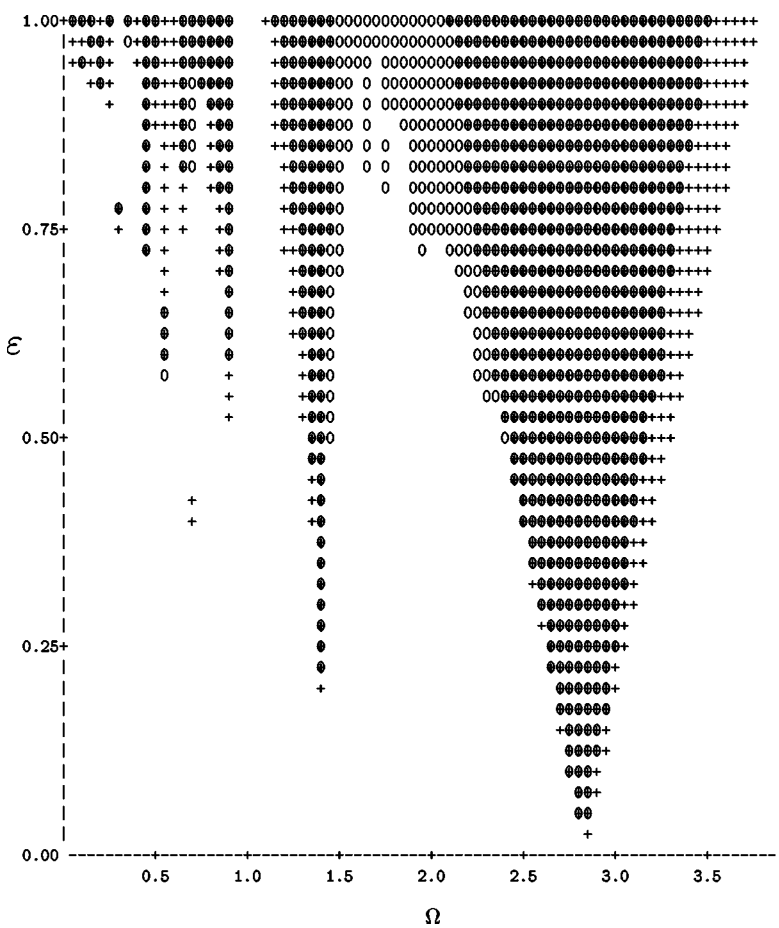

FIG. 4. Instability zones, as found from direct simulations of the Gross-Pitaevskii equation (4). In the area covered by open circles, the oscillating soliton develops an intrinsic instability, in the form of a growing amplitude of the internal vibrations. Shown by crosses are regions where the soliton demonstrates external instability. The double parametric resonance occurs where both areas overlap. The dynamics is identified as unstable if the onset of the amplitude growth is detected during the simulation time, of up to $t \sim 1000$. In physical units, this time estimates the actual lifetime of the condensate, under experimentally realistic conditions.

the oscillatory motion of the soliton (*external instability*), and of the amplitude of its intrinsic vibrations (*intrinsic instability*), as shown in Fig. 3. In accordance with the fact that Eq. (11) is an exact corollary of Eq. (4), the onset of the external instability is observed precisely at frequencies where it is predicted by simulations of the linear Mathieu Eq. (11). In Fig. 3, one can see some difference between the oscillation law for $\xi(t)$ as found from the direct simulations of the GPE and from the numerical integration of the ODE (11). An explanation for this is that the soliton under periodic perturbation emits linear waves which are absorbed on the domain boundaries. This process is enhanced under parametric resonance, and as a result, the norm of the soliton slowly decreases (note that the Ehrenfest theorem presumes a constant norm). In the experiment, a similar role may be played by evaporation of atoms from a finite-size trap. Detuning from the resonance due to such mass loss can be explored by dint of soliton perturbation theory based on the inverse scattering transform [24], which should be a subject of separate consideration.

Instability zones found from direct simulations of the GPE (4) are presented in Fig. 4. To collect data for this figure, the simulations were run long enough (typically, up to $t\sim 1000$, which in physical units corresponds to the lifetime of the condensate, ~ 3 s), in a harmonic trap with the confining frequency $\omega_x \simeq 2\pi\times 50$ Hz. Such a long simulation time makes it possible to unambiguously distinguish between stable and unstable behaviors. A practical criterion for the onset of the instability was that the oscillation amplitude would grow, at least, by a factor of 5 in the course of the evolution.

The instability zones shown in Fig. 4 reveal three separate PRs, viz., the fundamental one at $\Omega=2.82$, obviously corresponding to $n=1$ in Eq. (14), and two higher-order PRs, at $\Omega=1.41$ and 0.94, which correspond to $n=2$ and 3, respectively. The instability growth rate rapidly decreases for higher-order resonances, which explains why the PRs corresponding to $n>3$ cannot be easily spotted by dint of direct simulations running for a finite time. This also explains the fact that the instability "tongues" corresponding to the PRs with $n=2$ and 3 do not extend to very small values of ε.

The borders of the intrinsic-instability zones reported in Fig. 4 are, generally, similar to the borders of the external instability (recall that the latter are strictly tantamount to the instability borders in the parametric plane of the ordinary ME), except for the notable upward shift of all the intrinsic-instability zones, including the one corresponding to the fundamental PR at $\Omega=2.82$. One reason for this shift is that, unlike the ODEs (11) and (10), in the GPE the oscillations of the soliton's position and, especially, its intrinsic vibrations give rise to emission of radiation. Although the emitted waves are almost invisible in the simulations (as mentioned above, they are absorbed at the edges of the computation domain), the radiation loss induces an effective dissipation in the system (which, in principle, can be accounted for in more sophisticated, but rather cumbersome, versions of the VA [25]). Then Eq. (10) will turn into a weakly damped nonlinear ME. It is known that weak friction indeed shifts the instability zones in the ME upward in ε, without affecting the resonant frequencies [26].

Finally, it is also relevant to stress that, although Fig. 4 displays what we define as instability zones, the soliton, even after the amplitude of its intrinsic vibrations starts to grow, does *not* feature self-destruction, remaining a coherent, although unsteady, object. Eventually, it gets destroyed, but only when it hits absorbers placed at the edges of the integration domain (as mentioned above, the absorbers emulate a real physical feature—a finite size of the experimental setup in which the BEC is trapped).

IV. COLLISIONS BETWEEN OSCILLATING SOLITONS

In the experiment, it may be quite feasible to create several solitons in one trap (which was actually done in Ref. [1]); therefore it is relevant to analyze the dynamics of a two-soliton state. As the solitons are expected to collide many times, systematic simulations of this configuration will also help to understand the nature of interactions between the matter-wave solitons.

The results of the investigation of two-soliton configurations can be summarized in a simple form: in all cases (both off-resonance and near-resonant ones), solitons easily survive multiple collisions, irrespective of the initial phase difference between them, which is evidence of the completely elastic character of the collisions. In particular, no tangible emission of radiation has been observed as a result of the collisions.

If the individual soliton does not get into an instability zone, then the periodically colliding pair (of identical solitons) remains stable as well. In the opposite case, when the soliton develops the instability by itself, the two solitons collide several times, while performing oscillations with a

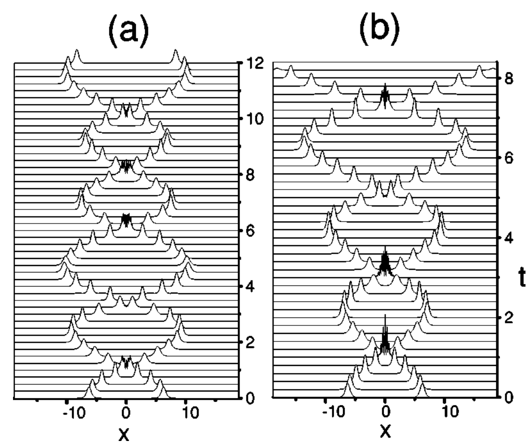

FIG. 5. Two solitons in the parabolic trap. (a) Multiple elastic collisions in the nonresonant case ($\varepsilon=0.5$, $\Omega=2.0$). (b) The case when the individual soliton falls into the instability zone induced by the fundamental parametric resonance (in this example, $\varepsilon=0.5$ and $\Omega=2.8$). In this case, the solitons elastically collide several times, performing oscillations with an increasing amplitude, and then get destroyed, hitting absorbers at the edges of the integration domain. In both cases (a) and (b), the Gross-Pitaevskii equation (4) was simulated with the initial configuration in the form of a pair of in-phase solitons $\psi_0(x)=\eta\{\mathrm{sech}[\eta(x-2\pi)]+\mathrm{sech}[\eta(x+2\pi)]\}$, with $\eta=2$.

growing amplitude. Eventually, both of them get destroyed, hitting the edge absorbers. Typical examples of this behavior are displayed in Fig. 5.

V. CONCLUSION

In this work, we have analyzed oscillatory motion of solitons in a quasi-1D self-attractive BEC, loaded into a parabolic potential trap, which is subjected to time-periodic "management." In the analytical approximation, the dynamics of the soliton is governed by the decoupled evolution equations for its center-of-mass coordinate $\xi(t)$ and width $a(t)$. The former is the linear Mathieu equation (which is an exact equation that does not depend on the adopted ansatz, as it follows from the Ehrenfest theorem), and the latter is a nonlinear version of the ME. Both equations give rise to the same map of instability zones (generated by parametric resonances of orders 1, 2, 3,…), in terms of the amplitude ε and frequency Ω of the periodic temporal modulation of the parabolic trap, if the instability is realized as permanent growth of the amplitude of the parametrically driven oscillations. Thus, double PR is expected in the system.

Direct simulations of the underlying Gross-Pitaevskii equation give rise to qualitatively similar, but quantitatively different instability maps for the intrinsic and external oscillations of the soliton. The double parametric resonance occurs in overlap areas of these two maps.

Two-soliton configurations were also investigated, with the conclusion that multiple collisions between solitons do not damage them. The collisions do not alter the borders of the instability zones either.

ACKNOWLEDGMENTS

B.B. thanks the Department of Physics at the University of Salerno (Italy) for a research grant. M.S. acknowledges partial financial support from the MIUR, through the interuniversity project PRIN-2003, and from the European LOCNET Grant No. HPRN-CT-1999-00163. B.M. appreciates the hospitality of the Department of Physics at Università di Salerno, and of the Department of Biological and Environmental Sciences at Università del Sannio (Benevento, Italy). The work of B.M. was partially supported by Grant No. 8006/03 from the Israel Science Foundation.

[1] K. E. Strecker, G. B. Partridge, A. G. Truscott, and R. G. Hulet, Nature (London) **417**, 150 (2002).
[2] L. Khaykovich, F. Schreck, G. Ferrari, T. Bourdel, J. Cubizolles, L. D. Carr, Y. Castin, and C. Salomon, Science **296**, 1290 (2002).
[3] L. D. Carr and J. Brand, Phys. Rev. Lett. **92**, 040401 (2004).
[4] H. Sakaguchi and B. A. Malomed, J. Phys. B **37**, 1442 (2004).
[5] H. Sakaguchi and B. A. Malomed, J. Phys. B **37**, 2225 (2004).
[6] J. J. García-Ripoll and V. M. Pérez-García, Phys. Rev. A **59**, 2220 (1999).
[7] J. J. García-Ripoll and V. M. Pérez-García, Phys. Rev. Lett. **83**, 1715 (1999).
[8] F. Kh. Abdullaev, R. M. Galimzyanov, M. Brtka, and R. A. Kraenkel, J. Phys. B **37**, 3535 (2004).
[9] F. Kh. Abdullaev and R. Galimzyanov, J. Phys. B **36**, 1099 (2003).
[10] F. Kh. Abdullaev and J. Garnier, Phys. Rev. A **70**, 053604 (2004).
[11] *Handbook of Mathematical Functions*, edited by M. Abramowitz and I. A. Stegun (Dover Publications, New York, 1965).
[12] T. F. Scott, R. J. Ballagh, and K. Burnett, J. Phys. B **31**, L329 (1998); V. M. Pérez-García, H. Michinel, and H. Herrero, Phys. Rev. A **57**, 3837 (1998); L. Salasnich, A. Parola, and L. Reatto, *ibid.* **65**, 043614 (2002); G. Theocharis, Z. Rapti, P. G. Kevrekidis, D. J. Frantzeskakis, and V. V. Konotop, *ibid.* **67**, 063610 (2003); J. J. Garcia-Ripoll, V. V. Konotop, B. Malomed, and V. M. Perez-Garcia, Math. Comput. Simul. **62**, 21 (2003).
[13] Y. B. Band, I. Towers, and B. A. Malomed, Phys. Rev. A **67**, 023602 (2003).
[14] G. Baym and C. J. Pethick, Phys. Rev. Lett. **76**, 6 (1996); F. Dalfovo, S. Giorgini, L. P. Pitaevskii, and S. Stringari, Rev. Mod. Phys. **71**, 463 (1999).
[15] P. A. Ruprecht, M. J. Holland, K. Burnett, and M. Edwards, Phys. Rev. A **51**, 4704 (1995); A. Eleftheriou and K. Huang, *ibid.* **61**, 043601 (2000).
[16] L. D. Carr and Y. Castin, Phys. Rev. A **66**, 063602 (2002).
[17] T. R. Taha and M. J. Ablowitz, J. Comput. Phys. **55**, 203 (1984).
[18] S. K. Adhikari and P. Muruganandam, J. Phys. B **35**, 2831 (2002).
[19] D. Anderson, Phys. Rev. A **27**, 3135 (1983); B. A. Malomed, Prog. Opt. **43**, 71 (2002).
[20] F. Kh. Abdullaev, J. C. Bronski, and G. Papanicolaou, Physica D **135**, 369 (2000).
[21] V. M. Perez-Garcia, P. Torres, J. J. Garcia-Ripoll, and H. Michinel, J. Opt. B: Quantum Semiclassical Opt. **2**, 353 (2000).
[22] R. Hasse, Phys. Rev. A **25**, 583 (1982).
[23] B. V. Chirikov, Phys. Rep. **52**, 263 (1979); A. J. Lichtenberg and M. A. Lieberman, *Regular and Stochastic Motion* (Springer-Verlag, New York, 1983).
[24] V. I. Karpman and E. M. Maslov, Zh. Eksp. Teor. Fiz. **75**, 504 (1978) [Sov. Phys. JETP **48**, 252 (1978)]; Yu. S. Kivshar and B. A. Malomed, Rev. Mod. Phys. **61**, 763 (1989).
[25] W. L. Kath and N. F. Smyth, Phys. Rev. E **51**, 1484 (1995).
[26] R. H. Rand, http://www.tam.cornell.edu/randdocs/nlvibe45.pdf.